Learned Optimizers for Analytic Continuation

Dongchen Huang[1,2] and Yi-feng Yang[1,2,3,*]

[1]*Beijing National Laboratory for Condensed Matter Physics and Institute of Physics,*
Chinese Academy of Sciences, Beijing 100190, China
[2]*University of Chinese Academy of Sciences, Beijing 100049, China*
[3]*Songshan Lake Materials Laboratory, Dongguan, Guangdong 523808, China*

(Dated: July 29, 2021)

Traditional maximum entropy and sparsity-based algorithms for analytic continuation often suffer from the ill-posed kernel matrix or demand tremendous computation time for parameter tuning. Here we propose a neural network method by convex optimization and replace the ill-posed inverse problem by a sequence of well-conditioned surrogate problems. After training, the learned optimizers are able to give a solution of high quality with low time cost and achieve higher parameter efficiency than heuristic full-connected networks. The output can also be used as a neural default model to improve the maximum entropy for better performance. Our methods may be easily extended to other high-dimensional inverse problems via large-scale pretraining.

Inverse problems appear in many perspectives of physics and machine learning, such as learning Hamiltonian in the classical [1–3] or quantum sense [4–6] and recovering sparse signal from noise measurements [7, 8]. In quantum many-body problems, correlation functions are often computed in imaginary time [9, 10] so that an analytic continuation has to be implemented to obtain the spectral function in real frequency in order to extract meaningful information. The analytic continuation is nothing but a linear inverse problem, which is, however, highly ill-posed and may often yield unphysical solutions.

Many algorithms have been proposed to attack this problem. These include padé approximation, stochastic methods [11–14], maximum entropy methods [15–21], and the Nevanlinna method [22]. Classical methods such as the padé approximation [23] and the singular value decomposition (SVD) [24] usually perform well in many tasks. The hyper parameter selection of maximum entropy methods can also be adjusted in various ways [25, 26]. But none of them holds for all situations and a case-by-case tuning is often needed. For instance, maximum entropy methods demand a highly empirical selection of prior distributions.

From the view of representation learning, high dimensional data of real world always have certain low-dimensional structures. The spectral function may have a sparse structure if it is properly discretized. This has motivated a line of work focusing on sparsity of the spectral function [27–31]. Unfortunately, the power of sparsity-based methods is greatly limited by the ill-poseness of the Fermi kernel matrix.

In this work, we develop a neural network architecture for analytic continuation by transforming a highly *ill-posed* basis pursuit problem into a sequence of *well-conditioned* surrogate problems. The problem sequence can be implemented by introducing a *learned optimizer* with given data, which may be viewed as a neural network whose structure can be directly derived from convex optimization. This neural network avoids empiri-

cal design and shows higher parameter efficiency compared with heuristic full-connected neural networks used in other works [32, 33]. It can give a high quality approximate solution of the linear inverse problem with much less time cost than traditional maximum entropy methods. Moreover, the two approaches can complement each other by taking advantage of neural network's strengths and treating its output as prior distributions of the maximum entropy, thus yielding an improved solution with better precision.

Analytic continuation. We are dealing with the inverse problem to obtain the spectral function $A(\omega)$ in real frequency from the Green's function $G(\tau)$,

$$G(\tau) = \int_{-\infty}^{\infty} K(\tau, \omega) A(\omega) d\omega, \qquad (1)$$

where τ is the imaginary time. For a fermionic Green's function, the kernel $K(\tau, \omega)$ takes the form,

$$K(\tau, \omega) = \frac{e^{-\tau \omega}}{1 + e^{-\beta \omega}}, \qquad (2)$$

where β is the inverse temperature. For analytic continuation, we first discretize Eq. (1) and get the linear inverse problem (in matrix form):

$$g(\tau_i) = K(\tau_i, \omega_j) a(\omega_j), \qquad (3)$$

where $i = 1, \ldots, N_\tau$ and $j = 1, \ldots, N_\omega$ mark the discrete points in imaginary time and real frequency, respectively, g is the vectorized Green's function, a is the vectorized spectral function, and $K(.,.)$ is a matrix of the Fermi kernel. The problem can then be solved using the Bayesian inference.

Maximum entropy and sparsity-based methods. The posterior distribution of the spectral function a satisfies the Bayes' theorem,

$$P(a|g) = \frac{P(g|a)P(a)}{P(g)}, \qquad (4)$$

from which a can be derived by maximum likelihood. The denominator $P(g)$ is independent of a and can be omitted in optimization. The maximum entropy and sparsity-based methods are two special forms of its implementation with different choices of $P(g|a)$ and $P(a)$.

The traditional maximum entropy methods choose $P(g|a) = -\chi^2/2$ and $P(a) \propto e^{-\alpha S}$, thus requiring

$$a = \arg\min_a \frac{\chi^2}{2} + \alpha S, \qquad (5)$$

where $\chi^2 = (g - Ka)^T \Sigma^{-1} (g - Ka)$ denotes the reconstruction error, Σ is the empirical covariance matrix, K is the kernel matrix, and $S = \sum_i \Delta\omega_i a(\omega_i) \log \frac{a(\omega_i)}{d(\omega_i)}$ is the Kullback-Leibler (KL) divergence between the spectral function and a prior default model $d(.)$.

The sparsity-based methods assume a Gaussian distribution with unit variance such that $P(g|a) \propto \exp(-\frac{1}{2}\|g - Ka\|_2^2)$. The prior distribution $P(a)$ is typically chosen by hand to reflect the sparse regularization. For Laplacian prior distribution, we have $P(a) \propto e^{-\lambda\|a\|_1} (\lambda > 0)$, where $\|.\|_1$ is the ℓ_1 norm defined as the summation of absolute values and λ is the hyperparameter. This leads to a basis pursuit (BP) problem,

$$a = \arg\min_a \frac{1}{2}\|g - Ka\|_2^2 + \lambda\|a\|_1. \qquad (6)$$

Ideally, ℓ_0 regularization should be used that counts the non-zero entries in a vector, but minimizing the ℓ_0 norm is NP-hard [34]. Fortunately, the ℓ_1 norm provides a good replacement which is the largest convex function to approximate ℓ_0. The sparsity assumption and such kind of problems have achieved huge amount of successes in machine learning and signal processing. The BP problem is well-posed and guaranteed to recovery the exact spectral function as long as a is sparse and the kernel matrix K satisfies some fine properties. The sparest solution is favored in this method, in contrast to maximum entropy methods that look for a solution of least deviation from the default model.

Solution of the BP problem. Since Eq. (6) is convex, many popular methods can be applied and all of them can converge to the only global minimum. Here we map it to the fixed-point problem [35],

$$a^* = S_{\tau\lambda}(a^* - \tau K^T(Ka^* - g)), \qquad (7)$$

where the soft-thresholding operator $S_{\tau\lambda}(.)$ is the proximal mapping of the function $\tau\lambda \|.\|_1$ and takes the form,

$$S_{\tau\lambda}(y) \equiv \begin{cases} y - \tau\lambda & y > \tau\lambda \\ 0 & |y| \leq \tau\lambda \\ y + \tau\lambda & y < -\tau\lambda \end{cases}. \qquad (8)$$

To see this, we note that a solution a^* of the BP problem must satisfy the optimality condition $0 \in K^T(Ka^* - g) + \lambda\partial \|a^*\|_1$, where $\partial(.)$ denotes the subdifferential.
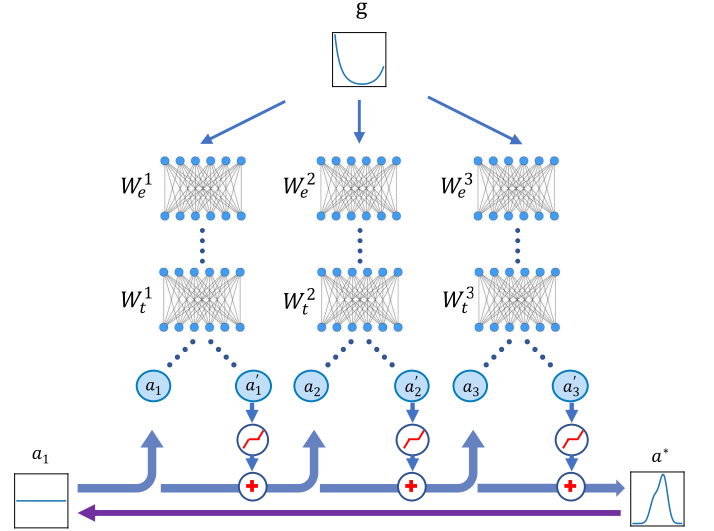

FIG. 1: Architecture of the 3-layer RLISTA network with input of the Green's function g and a zero vector a_1. The blue arrows illustrate the forward propagation of the optimization process, and the purple arrow indicates the backward propagation which tunes all parameters to feed the data.

Thus, for any $\tau > 0$, we have $a^* - \tau K^T(Ka^* - g) \in a^* + \tau\lambda\partial \|a^*\|_1$. On the other hand, for any convex function $F : \mathbb{R}^N \to (-\infty, \infty]$ and its induced proximal mapping $P_F(z) = \arg\min_x F(x) + \frac{1}{2}\|x - z\|_2^2$, the identity $x = P_F(z)$ implies $z \in x + \partial F(x)$. Combining these two immediately gives $F(x) = \tau\lambda \|x\|_1$ and the above fixed-point equations. It is now understood that the unit variance assumption in Eq. (6) corresponds to a convenient usage of the proximal mapping.

The fixed-point problem has a natural iteration scheme:

$$a_{n+1} = S_{\tau\lambda}(a_n - \tau K^T(Ka_n - g)), \qquad (9)$$

which is also called the iterative shrinkage-thresholding algorithm (ISTA) [36, 37]. Unfortunately, for analytic continuation, it fails to converge to the physical fixed point because of the ill-poseness of the Fermi kernel.

Learned optimizers. To overcome this issue, we note that ISTA can also be viewed as recurrent neural networks (RNNs) with fixed weights determined by the Fermi kernel matrix. This motivates us to design a neural network structure by unrolling the fixed-point iteration and utilize the simple forward problem of Eq. (3) to generate data, train the own weights for each individual layer, and learn an adaptive optimizer. We propose the following learnable iterative soft thresholding algorithm (LISTA) and its residual version (RLISTA) with a L-layer neural network of fixed depth:

$$\begin{aligned} a_{n+1} &= (1 - \eta)a_n + \eta S_{\tau\lambda}(W_t^n a_n + W_e^n g), \\ a_{n+1} &= S_{\tau\lambda}(W_t^n a_n + W_e^n g), \quad n = 1, 2, \ldots, L. \end{aligned} \qquad (10)$$
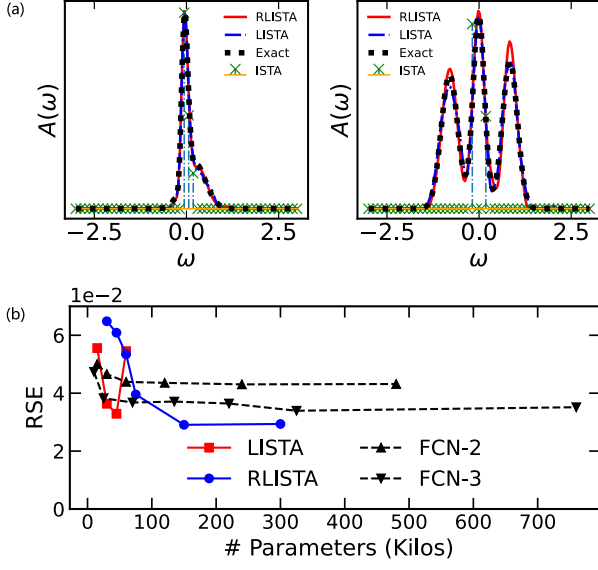
FIG. 2: (a): Comparison of RLISTA, LISTA and ISTA for simulated data generated from the spectral function with only one sharp peak (left) and more peaks (right). ISTA can only recover the single peak structure, while LISTA and RLISTA work well in both cases. (b) Comparison of parameter efficiency for four different neural network architectures: LISTA, RLISTA and fully-connected network of two (FCN-2) or three (FCN-3) layers.
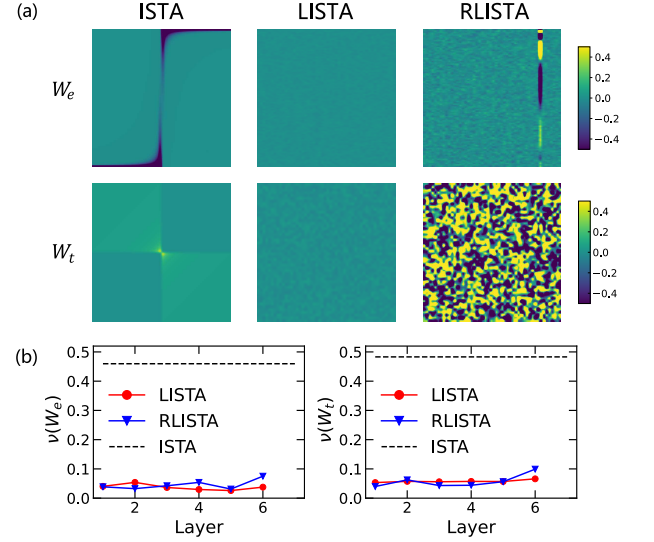

FIG. 3: (a) Comparison of the first layer matrices W_t and W_e in ISTA, LISTA and RLISTA optimizers. The color bars are normalized by their Frobenius norm $\|W_e\|_F^2$ and $\|W_t\|_F^2$. Before normalization, an identity matrix is subtracted from the matrix W_t, while the learned W_e and all matrices related to ISTA are multiplied by -1. (b) Comparison of the average coherence of their learned matrices for all layers, showing the benefits of learning in LISTA and RLISTA.

where a_1 and g are inputs of the neural network and $0 < \eta < 1$ is a relaxation factor. The parameters W_e^n and W_t^n represent the weights to be learned on the n-th layer to replace the fixed weights $W_e = \tau K^T$ and $W_t = I - \tau K^T K$ in the original problem. During the training and inference processes, the neural networks are fed with the Green's function g and a zero vector as a_1. The overall scheme is shown in Fig. 1 containing naturally a residual connection [38] and independent weights on each layer. We call the neural network RLISTANet. Historically, LISTA has been proposed for sparse coding [39].

Performance and parameter efficiency. Our learned optimizers, LISTA and RLISTA, have higher performance than vanilla ISTA, as compared in Fig. 2(a). For simple spectra with only one sharp peak near the origin, all three optimizers can recover the solution well. But for complex spectra containing more broad peaks, ISTA can only give a single sharp peak, while both LISTA and RLISTA can produce the ground truth with high accuracy.

Our neural networks may be viewed as a variation of the fully-connected network (FCN) but show higher parameter efficiency. This is seen by comparison with the conventional FCN of one or two hidden layers. For simplicity, the width of single FCN is set equal. The neural

performance is measured by the root square error (RSE),

$$\text{RSE}(\hat{a}) = \sqrt{\sum_{i=1}^{N_\omega} (a_i^* - \hat{a}_i)^2}, \tag{11}$$

where a^* is the ground truth spectral function in the test set and $\hat{a}$ is the prediction of the neural network. As shown in Fig. 2(b), our 6-layer LISTANet can already achieve better accuracy than 2-layer FCN of ten times more parameters and 3-layer FCN of seven times more parameters. However, deeper LISTANet does not necessarily outperform shallow ones, possibly due to the landscape of networks [40]. Deep FCNs are known difficult to train and require more advanced techniques like normalization [41–43]. By contrast, RLISTA contains residual connection [38] and allows for the training of much deeper networks. Although shallow RLISTA cannot outperform LISTA, we can always train a deeper (40-layer) RLISTA that beats all other three. However, when the depth is larger than 20, adding layers no longer reduces the error, reflecting a possible bottleneck of RLISTA. Relaxation methods are usually known to accelerate convergence and improve stability. Exploring the connection between acceleration and convergence conditions and the landscape of corresponding neural networks may be beneficial for designing better architecture and optimization techniques and help improve the performance and achieve better accuracy.

The weight matrices. What is the reason behind the substantial improvement in learned optimizers? Noticing that ISTA may be viewed as an infinite-layer neural network with fixed weight, the improvement must originate from the adaptation to the data as reflected in the learned weight matrices. Figure 3 compares the normalized learned matrices W_t and W_e on first layer for different optimizers. While the matrices in ISTA are determined directly by the Fermi kernel, the learned matrices in LISTA and RLISTA are heavily influenced by their different iteration schemes. All entries of W_e in LISTA distribute uniformly and are of the same magnitude, while those in RLISTA differ heavily and contain some entries of relatively larger values. Nevertheless, both types of learned matrices can empirically solve the inverse problem and perform nicer than their vanilla cousin ISTA.

To quantify the "niceness" of the learned matrices, we use the average coherence [44, 45] for a matrix $A = [a_1 | \ldots | a_n] \in \mathbb{R}^{m \times n}$:

$$\nu(A) = \frac{1}{n-1} \max_{i \in \{1,\ldots,n\}} \Big| \sum_{j \neq i, j=1}^{n} \Big\langle \frac{a_i}{\|a_i\|_2}, \frac{a_j}{\|a_j\|_2} \Big\rangle \Big|, \quad (12)$$

which gives the largest average inner product of two columns and measures the spread of column vectors of a matrix within a unit ball. The average coherence values in $[0, 1]$, becomes zero for an orthogonal matrix, and reaches its upper bound for a matrix with repeated columns. Obviously, a lower average coherence implies a "nicer" or less singular matrix. As shown in Fig. 3, the average coherence of learned matrices values around the lower bound zero, while the predefined matrices in ISTA have a large average coherence close to 0.5. The gap between them illustrates the benefits of learning.

The diversity of learned matrices in different optimizers might be understood as the diversity of learned problems. Each layer of LISTA and RLISTA networks works approximately as an independent iteration step for solving a given BP problem of Eq. (6) with their individual learned kernel matrix. But a single iteration can not solve the problem with high accuracy. With many learned layers, the neural networks learn a sequence of optimization problems and solve each of them imprecisely.

From the perspective of optimization, our method may be understood as a generalization of the classical homotopy method [46] which solves the BP problem by a sequence of problems with varying regularization parameter λ. Here the neural network solves the problem by a series of problems with varying K and λ in the region of physical Green's functions, which is much smaller than the whole space $\mathbb{R}^{N_\tau}$. Thus, a trade-off comes from the fixed depth: how precisely do we need to solve a single question (precision) and how many optimization problems do we need to learn (diversity)? Careful studies of the precision-diversity trade-off may reveal a closer relationship between optimization and neural network, which
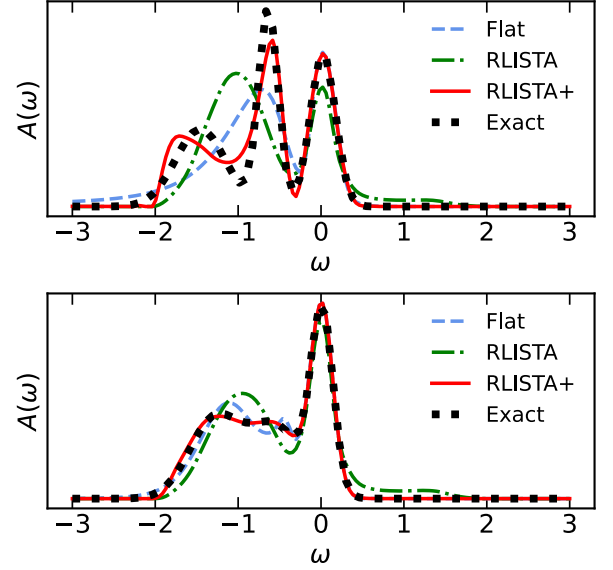

FIG. 4: Two examples comparing the maximum entropy method with a flat default model (Flat) and a neural default model (RLISTA+). The dots are the ground truth spectral function. The RLISTA results are generated by a sub-optimal 6-layer network.

we leave for future work.

A neural default model. The neural networks can give an answer with low time cost after training, but they are often criticized as being a "black-box", where precise interpretations of the weights remain unclear. Better neural network architectures and optimization techniques can no doubt reduce the error, but their design suffers from high cost trial and error. On the other hand, a classical maximum entropy problem requires a default model $d(\omega)$ to incorporate certain prior knowledge about the desired spectral function. A better default model allows for easy hyperparameter tuning and gives better accuracy. We propose that combining the two may provide a novel way to improve the performance. The output of our neural network is also a probability distribution and may be considered as a "neural default model" required in the maximum entropy. This fixes the inexactness of the neural network and can benefit from both the high speed of neural networks and the well-developed algorithms of the maximum entropy.

To get an impression on the advantage of such combination, we first obtain an inexact result from a sub-optimal 6-layer RLISTA. Figure 4 shows two examples where both neural network and maximum entropy (with flat prior) cannot capture all the details of the spectral function. While the neural network tends to average two peaks, the maximum entropy method ignores the peak at high frequency. By contrast, using the neural default model, the maximum entropy solution can capture well the high frequency peak and even all the details of

the exact spectral function. This neural maximum entropy method (RLISTA+) makes a promising improvement over the conventional one for analytic continuation.

Discussion and conclusions. Motivated by sparsity-based methods, we have proposed a highly efficient neural network scheme for analytic continuation in quantum many-body problems. Our learned optimizers show low time costs and may be easily extended to other high-dimensional inverse problems via large-scale pre-training where traditional maximum entropy methods demand tremendous computation time. The output of our method may also be used as a neural default model to improve the performance of maximum entropy methods and make use of their both advantages. We also find that constructing neural networks from fix-point iteration can achieve better parameter efficiency than heuristic full-connected networks. By viewing neural network as learnable fix-point iteration, we see that different fix-point iteration schemes are not equivalent if their parameters can be learned, despite that they all converge to the same solution for a given problem. The learned iteration paths are more regular than their unlearned counterpart. This, combined with the powerful theory about calculus of variations, may help invent novel algorithms and lead to a better understanding of the training dynamics and regularization of neural networks.

* yifeng@iphy.ac.cn

[1] C. Chow and C. Liu, Approximating discrete probability distributions with dependence trees, IEEE Transactions on Information Theory, **14**. 462 (1968).

[2] G. E. Hinton and T. J. Sejnowski, *Learning and Relearning in Boltzmann Machines*, p. 282–317. Cambridge, MA, USA: MIT Press, 1986.

[3] G. Bresler, Efficiently learning Ising models on arbitrary graphs, in *STOC'15*, (New York, NY, USA), Association for Computing Machinery, 2015.

[4] A. Anshu, S. Arunachalam, T. Kuwahara, and M. Soleimanifar, Sample-efficient learning of quantum many-body systems, in *2020 IEEE 61st Annual Symposium on Foundations of Computer Science (FOCS)*, (2020).

[5] E. Bairey, I. Arad, and N. H. Lindner, Learning a local Hamiltonian from local measurements, Phys. Rev. Lett. **122**. 020504 (2019).

[6] M. H. Amin, E. Andriyash, J. Rolfe, B. Kulchytskyy, and R. Melko, Quantum Boltzmann machine, Phys. Rev. X **8**. 021050 (2018).

[7] D. Donoho, M. Elad, and V. Temlyakov, Stable recovery of sparse overcomplete representations in the presence of noise, IEEE Transactions on Information Theory, **52**. 6 (2006).

[8] E. Candes, M. Rudelson, T. Tao, and R. Vershynin, Error correction via linear programming, in *46th Annual IEEE Symposium on Foundations of Computer Science (FOCS'05)*, (2005).

[9] E. Gull, A. J. Millis, A. I. Lichtenstein, A. N. Rubtsov, M. Troyer, and P. Werner, Continuous-time Monte Carlo methods for quantum impurity models, Rev. Mod. Phys. **83**. 349 (2011).

[10] J. Gubernatis, N. Kawashima, and P. Werner, Quantum Monte Carlo Methods: Algorithms for Lattice Models. Cambridge University Press, 2016.

[11] A. W. Sandvik, Stochastic method for analytic continuation of quantum monte carlo data, Phys. Rev. B **57**. 10287 (1998).

[12] A. W. Sandvik, Constrained sampling method for analytic continuation, Phys. Rev. E **94**. 063308 (2016).

[13] K. Ghanem and E. Koch, Average spectrum method for analytic continuation: Efficient blocked-mode sampling and dependence on the discretization grid, Phys. Rev. B **101**. 085111 (2020).

[14] K. Ghanem and E. Koch, Extending the average spectrum method: Grid point sampling and density averaging, Phys. Rev. B **102**. 035114, 2020.

[15] M. Jarrell and J. Gubernatis, Bayesian inference and the analytic continuation of imaginary-time quantum Monte Carlo data, Physics Reports, **269**. 133 (1996).

[16] J.-H. Sim and M. J. Han, Maximum quantum entropy method, Phys. Rev. B, **98**. 205102 (2018).

[17] G. J. Kraberger, R. Triebl, M. Zingl, and M. Aichhorn, Maximum entropy formalism for the analytic continuation of matrix-valued Green's functions, Phys. Rev. B **96**. 155128 (2017).

[18] R. N. Silver, D. S. Sivia, and J. E. Gubernatis, Maximum-entropy method for analytic continuation of quantum Monte Carlo data, Phys. Rev. B **41**. 2380 (1990).

[19] O. Gunnarsson, M. W. Haverkort, and G. Sangiovanni, Analytical continuation of imaginary axis data using maximum entropy, Phys. Rev. B **81**. 155107 (2010).

[20] A. Reymbaut, D. Bergeron, and A.-M. S. Tremblay, Maximum entropy analytic continuation for spectral functions with nonpositive spectral weight, Phys. Rev. B **92**. 060509 (2015).

[21] M. Rumetshofer, D. Bauernfeind, and W. von der Linden, Bayesian parametric analytic continuation of Green's functions, Phys. Rev. B **100**. 075137 (2019).

[22] J. Fei, C.-N. Yeh, and E. Gull, Nevanlinna analytical continuation, Phys. Rev. Lett. **126**. 056402 (2021).

[23] J. J. Deisz, D. W. Hess, and J. W. Serene, Incipient antiferromagnetism and low-energy excitations in the half-filled two-dimensional Hubbard model, Phys. Rev. Lett. **76**. 1312 (1996).

[24] O. Gunnarsson, M. W. Haverkort, and G. Sangiovanni, Analytical continuation of imaginary axis data for optical conductivity, Phys. Rev. B **82**. 165125 (2010).

[25] R. K. Bryan, Solving Oversampled Data Problems By Maximum Entropy, pp. 221–232. Dordrecht: Springer Netherlands, 1990.

[26] D. Bergeron and A.-M. S. Tremblay, Algorithms for optimized maximum entropy and diagnostic tools for analytic

continuation, Phys. Rev. E **94**. 023303 (2016).

[27] M. Ohzeki, Sparse modeling for quantum Monte-Carlo simulation, Journal of Physics: Conference Series, **1036**. 012020 (2018).

[28] K. Yoshimi, J. Otsuki, Y. Motoyama, M. Ohzeki, and H. Shinaoka, "Spm: Sparse modeling tool for analytic continuation of imaginary-time Green's function," Computer Physics Communications, **244**. 319 (2019).

[29] J. Otsuki, M. Ohzeki, H. Shinaoka, and K. Yoshimi, Sparse modeling in quantum many-body problems, Journal of the Physical Society of Japan, **89**. 012001 (2020).

[30] J. Otsuki, M. Ohzeki, H. Shinaoka, and K. Yoshimi, Sparse modeling approach to analytical continuation of imaginary-time quantum Monte Carlo data, Phys. Rev. E, **95**. 061302 (2017).

[31] H. Shinaoka, J. Otsuki, M. Ohzeki, and K. Yoshimi, "Compressing Green's function using intermediate representation between imaginary-time and real-frequency domains," Phys. Rev. B **96**. 035147 (2017).

[32] R. Fournier, L. Wang, O. V. Yazyev, and Q. Wu, Artificial neural network approach to the analytic continuation problem, Phys. Rev. Lett. **124**. 056401 (2020).

[33] H. Yoon, J.-H. Sim, and M. J. Han, Analytic continuation via domain knowledge free machine learning, Phys. Rev. B **98**. 245101 (2018).

[34] B. K. Natarajan, "Sparse approximate solutions to linear systems," SIAM J. Comput., **24**. 227 (1995).

[35] S. Boyd and L. Vandenberghe, Convex Optimization. Cambridge University Press, 2004.

[36] I. Daubechies, M. Defrise, and C. De Mol, An iterative thresholding algorithm for linear inverse problems with a sparsity constraint, Communications on Pure and Applied Mathematics, **57**. 1413 (2004).

[37] M. Figueiredo and R. Nowak, An EM algorithm for wavelet-based image restoration, IEEE Transactions on Image Processing, **12**. 906 2003.

[38] K. He, X. Zhang, S. Ren, and J. Sun, Deep residual learning for image recognition, in *2016 IEEE Conference on Computer Vision and Pattern Recognition (CVPR)*, (2016).

[39] K. Gregor and Y. LeCun, Learning fast approximations of sparse coding, in *Proceedings of the 27th International Conference on Machine Learning* (2010).

[40] H. Li, Z. Xu, G. Taylor, C. Studer, and T. Goldstein, "Visualizing the loss landscape of neural nets," in *Advances in Neural Information Processing Systems* (S. Bengio, H. Wallach, H. Larochelle, K. Grauman, N. Cesa-Bianchi, and R. Garnett, eds.), vol. 31, Curran Associates, Inc., 2018.

[41] S. Ioffe and C. Szegedy, "Batch normalization: Accelerating deep network training by reducing internal covariate shift," in *Proceedings of the 32nd International Conference on Machine Learning*, (F. Bach and D. Blei, eds.) vol. 37 of *Proceedings of Machine Learning Research*, (Lille, France), pp. 448–456, PMLR, 2015.

[42] J. Ba, J. Kiros, and G. E. Hinton, Layer normalization, arXiv:1607.06450, (2016).

[43] Y. Wu and K. He, "Group normalization," in *Computer Vision – ECCV 2018* (V. Ferrari, M. Hebert, C. Sminchisescu, and Y. Weiss, eds.), pp. 3–19, Springer International Publishing, 2018.

[44] W. U. Bajwa, R. Calderbank, and S. Jafarpour, "Why gabor frames? Two fundamental measures of coherence and their role in model selection," Journal of Communications and Networks, **12**. 289 (2010).

[45] D. G. Mixon, W. U. Bajwa, and R. Calderbank, "Frame coherence and sparse signal processing," in *2011 IEEE International Symposium on Information Theory Proceedings*, (2011)

[46] D. L. Donoho and Y. Tsaig, "Fast solution of ℓ_1-norm minimization problems when the solution may be sparse," IEEE Transactions on Information Theory, **54**. 4789 (2008).